Reactive-environment, hollow cathode sputtering: basic characteristics and application to Al_2O_3, doped ZnO, and In_2O_3:Mo

A. E. Delahoy[a] and S. Y. Guo
Energy Photovoltaics, Inc., Lawrenceville, New Jersey 08648

C. Paduraru and A. Belkind
Department of Physics, Stevens Institute of Technology, Hoboken, New Jersey 07030

(Received 15 October 2003; accepted 1 March 2004)

A method for thin-film deposition has been studied. The method is based on metal sputtering in a hollow cathode configuration with supply of a reactive gas in the vicinity of the substrate. The working gas and entrained sputtered atoms exit the cathode through an elongated slot. The reactive gas is thereby largely prevented from reaching the target. The basic operation of the cathode was studied using a Cu target and pulsed power excitation. These studies included the dependence of deposition rate on power, pressure, and flow rate, film thickness profiles, and film resistivity as a function of substrate conditions. Modeling was conducted to calculate the gas velocity distribution and pressure inside the cavity. Al_2O_3 films were prepared in a reactive environment of oxygen by sputtering an Al target. It was demonstrated that only a very small amount of oxygen passing *through* the cathode will oxidize (poison) the target, whereas large quantities of oxygen supplied *externally* to the cathode need not affect the target at all. A very stable discharge and ease of Al_2O_3 formation were realized in this latter mode. The method was applied to the preparation of transparent, conductive films of ZnO doped with either Al or B. High deposition rates were achieved, and, at appropriate oxygen flow rates, low film resistivities. High-mobility In_2O_3:Mo transparent conductors were also prepared, with resistivities as low as $1.9\times10^{-4}\,\Omega$ cm. Scaling relations for hollow cathodes, and deposition efficiency, and process comparisons between magnetron sputtering and linear, reactive-environment, hollow cathode sputtering are presented.
 [DOI: 10.1116/1.1723289]

I. INTRODUCTION

Sputtering is a convenient and widely used method for thin-film deposition. To increase the deposition rate, magnetron sputtering is usually employed. In this method, the electron density (and hence ion production) near the target is increased by magnetic confinement. The deposition of metals is straightforward, but the use of reactive magnetron sputtering to prepare metal oxides and other compound films is accompanied by practical problems stemming from the chemical reaction of the reactive gas (e.g., oxygen) with the target material. One consequence can be a hysteresis loop for deposition rate versus oxygen flow, reflecting the oxidation state of the target. The difficulties become severe if all or parts of the target surface are rendered electrically insulating. These effects lead to low deposition rate, plasma instabilities, and arcing. Furthermore, because the target is eroded in a racetrack pattern, target utilization is poor.

Another method of increasing the plasma density is to utilize a hollow cathode (HC) discharge. Particularly intense plasmas can be sustained inside a cavity in the cathode material through geometrical and electrostatic confinement of electrons, and reduced ion loss. Secondary electrons, as well as electrons created in the sheath, are accelerated by the electric field in the cathode sheath, and these fast electrons may oscillate back and forth between opposing cathode surfaces, being reflected each time by the cathode fall.[1] Each electron may ionize a large number of working gas atoms (e.g., Ar) before being lost. The plasma density is much higher than that for a planar cathode, and comparable to that of a magnetron cathode. The resulting Ar^+ ions bombard and sputter the interior of the cathode. If it is arranged that the Ar flows through the cavity, then some of the sputtered atoms are entrained and carried out of the cavity by the Ar flow. The atoms may then be deposited upon a substrate. This method of film deposition, termed gas flow sputtering, and with a cylindrical tube used as the HC, was presented by Ishii.[2]

Aware of Ishii's work, we conceived a linearly extended cavity for coating moving substrates by hollow cathode sputtering (HCS), and initiated an experimental program. We later learnt of similar German efforts.[3–5] The program at Energy Photovoltaics was motivated by various schemes for processing in a reactive environment (RE), that is, the sputtering of a target material in a chamber containing a gaseous atmosphere that would normally react with the target material. It was envisaged that a sufficiently high flow of the working gas through the cathode cavity would prevent backstreaming of the reactive gas into the cavity, thereby eliminating target poisoning. To distinguish this process from conventional reactive sputtering (in which the reactive gas has access to the target) we term this process *reactive-environment sputtering*.

In this article, we report our investigation of HCS performed with a linear HC source operated with midfrequency

[a]Electronic mail: a.delahoy@epv.net

TABLE I. Cathode dimensions and typical operating parameters.

Dimension/parameter	Value
Cathode length (internal)	9.91 cm
Cathode depth	4.06 cm
Slot width	1.27 cm
Cathode surface area	90.8 cm^2
Sputtering power	50–1400 W
Frequency	50–100 kHz
Power density	0.55–15.4 W cm^{-2}
Gas flow	2000–6000 sccm
Gas velocity (peak)	256–770 m s^{-1}
Chamber pressure	100–500 mTorr
Pressure in cathode (average)	300–750 mTorr

pulsed power. Deposition of thin films of Cu, Al, Zn, and In were performed to study properties of the source for simple metal sputtering. Using Cu, the effect of deposition parameters on deposition rate and film quality was studied experimentally. For further understanding, the Ar velocity distribution in the cavity and the pressure differential as a function of flow rate were calculated. Because of the high reactivity of Al and oxygen and the insulating nature of the oxide, Al_2O_3 deposition was performed to exhibit the advantages of the RE sputtering method. Rate studies and optical emission were used to study whether oxygen penetrated the cathode under various process conditions. RE-HCS was also utilized to deposit oxides such as ZnO and In_2O_3. With the introduction of suitable dopants, and appropriate choice of deposition conditions, transparent conducting oxides (TCOs) with excellent properties were produced. In the context of large-area TCO deposition, a comparison was made between conventional magnetron sputtering and linear RE-HCS.

II. EXPERIMENT

At Energy Photovoltaics, Inc., (EPV), depositions were performed in a custom-built, rectangular vacuum system in which was mounted a linear, HCS source having a 10 cm exit slot. A molecular drag pump was used for pumping to high vacuum. The process pump consists of a mechanical booster/rotary pump combination having a pumping speed of 1000 $m^3 h^{-1}$. Provision is made for introducing argon (99.9999%) as the working gas, as well as other reactive gases. The flow rates are set using mass flow controllers. The chamber pressure is set using a throttling gate valve and measured using a capacitance manometer. A midfrequency, bipolar, pulsed plasma generator (5 kW) is used as the power supply for the cathode. The supply was mostly used in constant power mode, the frequency being set in the range 50 to 100 kHz. For convenience, typical dimensions and operating parameters for the cathode are summarized in Table I.

The HCS source is shown schematically in Fig. 1, as is the overall geometric configuration of source, substrate, gas injection, and pumping. Target pieces are mounted on a water-cooled Cu cathode block and define the dimensions of the cathode cavity. The argon is introduced through a linear manifold mounted behind the entrance to the cavity and is constrained to flow through the cavity. For operation in a

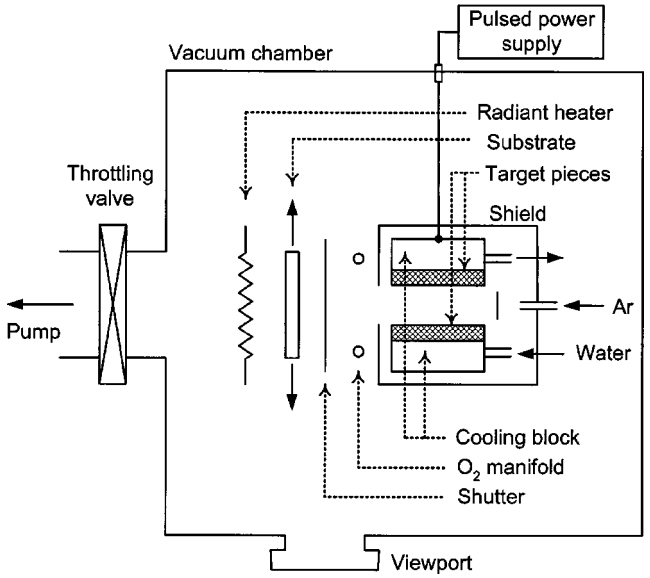

FIG. 1. Schematic diagram of RE sputtering system with linear, HC source.

reactive mode, the reactive gas is introduced through a manifold mounted externally to the cathode and in front of the dark shield. The substrates for thin-film deposition are generally 13.0 cm×10.1 cm pieces of 3-mm-thick soda-lime glass. Prior to each deposition, the target is presputtered with a shutter covering the substrate. Depositions are performed either in static mode or with slow substrate translation. Three 550 W IR lamps are available for substrate heating. With no substrate in place, the local deposition rate can be measured using a quartz crystal monitor (QCM) mounted in the center of the substrate holder. The total film mass deposited on the substrate was determined by weighing the substrate before and after deposition. The local film thickness and sheet resistance were measured by stylus profilometer and four-point probe, respectively. Dopant concentrations in TCOs were measured by inductively coupled plasma (ICP) optical emission spectroscopy (Varian Liberty II) calibrated using standard solutions of the host and dopant metals.

At Stevens Institute of Technology, a HC with cavity dimensions 3.17 cm×0.63 cm×2.54 cm was installed in a six-way-cross vacuum chamber.[6,7] Time-resolved optical emission data were acquired using a photomultiplier and a Tektronix™ TDS3034 digital oscilloscope. The line of sight was perpendicular to the emission axis of the cathode and aligned with the exit slot. Except where otherwise noted, the data in this article were obtained using the EPV HC system.

III. RESULTS AND DISCUSSION

A. Cathode and deposition characteristics

Typical discharge I–V curves of the HC fitted with Cu target pieces and using Ar as the working gas are shown in Fig. 2. At a given flow rate and discharge current, the required discharge voltage is higher at lower pressures. At a given chamber pressure, the I–V characteristics at two different flow rates are very similar, the voltage for a given

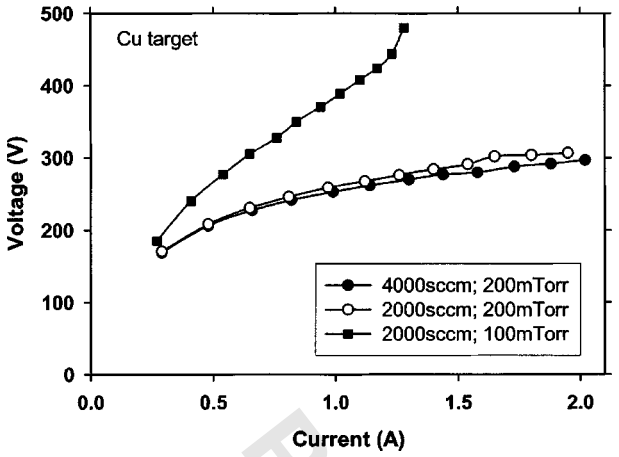

FIG. 2. HC $I-V$ curve at different flow rates and pressures.

current being slightly higher at the higher flow rate. This difference results from the increase with flow rate of the elevated pressure inside the HC.

The main factors determining the peak local deposition rate were shown to be discharge power, the flow rate of the working gas, and the source-to-substrate distance. Figure 3 shows the dependence of Cu deposition rate, measured by QCM at a distance of 3.5 cm, on power, for a fixed flow rate of 5000 sccm and a pressure of 286 mTorr. The deposition rate was found to depend linearly on power, with rates in the neighborhood of 200 $\text{Å}\,\text{s}^{-1}$ being obtained at a discharge power of 1.4 kW. In order to measure the effective deposition rate as a function of flow rate, the total film mass deposited on the substrate was determined by weighing. This approach is necessary because the thickness profile depends on flow rate. Figure 3 shows the mass of Cu deposited per minute versus Ar flow rate at 1 kW and 660 mTorr. Between 1000 and 3000 sccm, the mass rate rises roughly linearly with flow rate, implying the sputtered atoms are being carried out of the cathode more effectively and redeposition is being reduced. The mass rate peaks at 23.5 $\text{mg}\,\text{min}^{-1}$ around

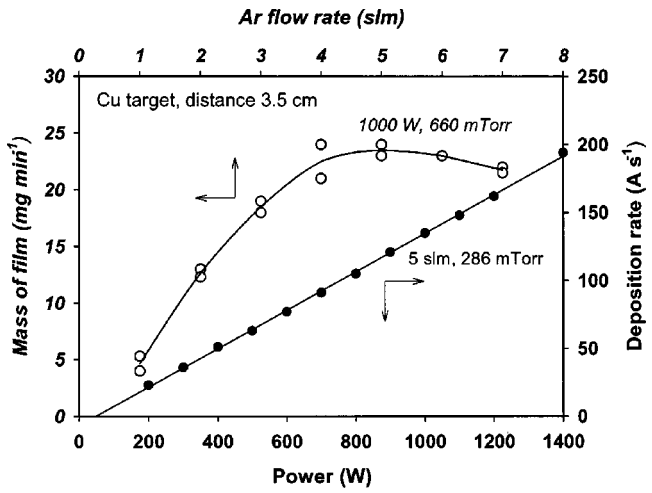

FIG. 3. Local deposition rate for Cu versus sputtering power, and total mass rate versus Ar flow.

TABLE II. Typical discharge conditions, rates, and yields for different metals (300 mTorr, 4 slm Ar).

Metal	Power (W)	Voltage (V)	Current (A)	Mass rate ($\text{mg}\,\text{min}^{-1}$)	App. yield (10^{-9} moles $\text{W}^{-1}\,\text{min}^{-1}$)
Cu	1000	372	2.68	30	0.47
Al	1000	303	3.30	2.5	0.093
Zn	300	450	0.66	5.4	0.28

5000 sccm, and then slowly declines to 17 $\text{mg}\,\text{min}^{-1}$ at 15 000 sccm (point not shown). At such very high flows, it seems that some of the Cu atoms are carried away before they reach or attach to the substrate. Pressure was found to be a secondary factor in determining mass rate. Thus, at 1 kW, 4000 sccm, and 3.5 cm, the mass rate declined by 22% upon raising the pressure from 300 to 660 mTorr.

Because of the high operating pressure of gas flow HCS, the sputtered atoms thermalize in the working gas and arrive at the substrate with very low kinetic energy.[2] In addition, if the substrate is located outside of the plasma zone, ion bombardment may be negligible. On the other hand, the mobility of atoms on the substrate surface can be increased by heating the substrate, by applying a negative bias to extract ions from the plasma and induce ion bombardment, or both. We have found the resistivity of Cu films to depend strongly on these effects. Thus, the resistivity, which is 8.5 $\mu\Omega\,\text{cm}$ on unheated, unbiased substrates, was reduced to 4.2 $\mu\Omega\,\text{cm}$ using a bias of -30 V, and to 2.4 $\mu\Omega\,\text{cm}$ at $T_s = 70\,^{\circ}\text{C}$ and -30 V.

The apparent sputtering yields obtained for Cu, Al, and Zn targets were calculated from the equation: apparent yield = mass rate/(power × atomic weight). Typical data for these targets, and the resulting yields (moles/W/min) are shown in Table II. The apparent yield is not equal to the conventional sputtering yield because of redeposition or transport losses. Nevertheless, the trends are similar.

The deposition thickness profile on a stationary substrate is an image of the geometry of the exit slot, but with broadening due to gas flow effects. Figure 4 shows several of these profiles in the longitudinal (long axis) and transverse (short axis) directions. With a source–substrate separation of just 2.2 cm, and with Cu targets on all four cavity faces, the longitudinal distribution drops sharply beyond the ends of the 10-cm-long source (700 W, 6000 sccm, 280 mTorr, 6 min). The peaks in thickness at ± 4 cm from the center suggest that a more intense plasma exists near the ends of the slot as a result of improved particle generation and confinement. The transverse profile shows a full width at half-maximum of about 3 cm. For a source–substrate separation of 6.5 cm a broader and flatter transverse distribution is obtained.

Depositions were also conducted with two Zn targets attached to the two large opposing faces of the cavity, and with either two Zn or two ceramic pieces (end blocks) attached to the two small end faces. The parameters were 300 W, 2000 sccm, 500 mTorr, 20 min, and a separation of 3.5 cm. With four Zn target pieces and these parameters, the end-effect

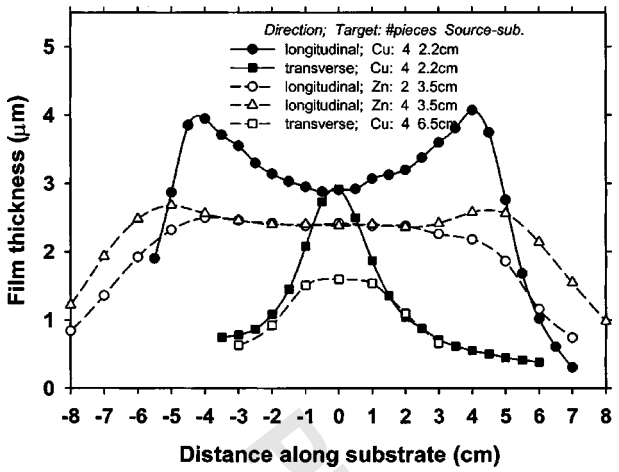

FIG. 4. Film thickness distribution in longitudinal and transverse directions for Cu and Zn films sputtered with different target configurations and source–substrate separations.

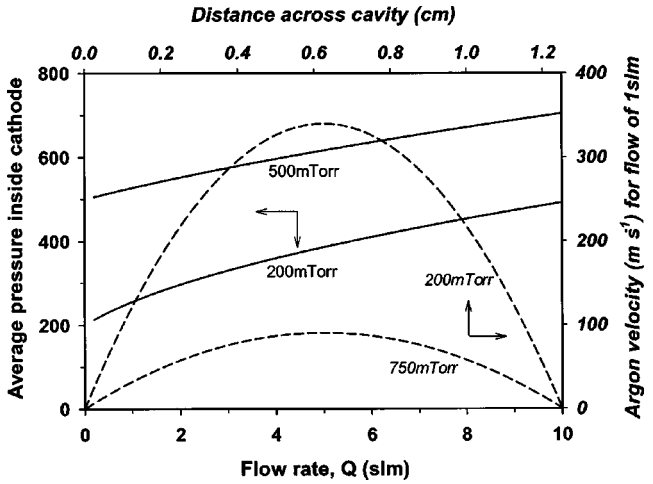

FIG. 5. Average pressure inside cathode cavity as a function of argon flow rate, and gas velocity distribution across the cavity, both calculated for two different chamber pressures.

peaks are less pronounced. With two Zn target pieces, the peaks disappear entirely (Fig. 4).

Plasma parameters were measured 3 cm away from the source exit using Langmuir probes. A planar single probe was used with a Cu target operated at 500 W, 2 slm Ar, and 400 mTorr. The measured remote plasma density opposite the source center was $2.15\times10^{11}\,\mathrm{cm}^{-3}$ and the electron temperature was 3.05 eV. The floating potential and the plasma potential were -2.3 and 10.0 V, respectively. The saturated ion current density was 4.0 mA/cm^2. Using a commercial, automated Langmuir probe with a 0.5 mm Ni wire, spatially resolved measurements were made in the longitudinal direction of the source at different pressures. The target material was In (four pieces), and the discharge parameters were 100 W, 3 slm Ar. At high pressures (800 mTorr), the distribution showed two peaks with a strong depression in the center, suggesting enhanced trapping at the ends of the cavity results in an amplified ion production rate. As the pressure was reduced to 200 mTorr, the depression in the center gradually disappeared.

B. Calculation of gas parameters inside the hollow cathode

In this section, we calculate the argon velocity distribution and the average pressure inside a rectangular hollow cathode having dimensions h, k, l, where h is the exit slot width, k is the exit slot length, and l is the depth. With Ar passing through the cathode, the gas speed is largest in the center of the cavity and is zero at the edge because of friction. For an Ar flow of 2 slm and an estimated gas temperature T_g inside the cathode of 600 K, the calculated Reynolds number is 34, and we suppose the gas flow to be laminar. Since $k\gg h$, we assume the gas velocity to be constant in the longitudinal direction. The gas velocity in the transverse direction x in a laminar shear is

$$W(x)=\frac{V_0\Delta P(hx-x^2)}{2l\nu}, \tag{1}$$

where ΔP is the difference of inlet pressure P_2 and outlet pressure P_1 of the hollow cathode, ν is the gas viscosity, and V_0 the specific volume. For Ar, $\nu=1.34\times10^{-5}\,\mathrm{m}^2/\mathrm{s}$, while at $P_0=760$ Torr, $T=293.15$ K, and $V_0=0.602\,\mathrm{m}^3/\mathrm{kg}$. By integrating the mass flow through the cavity, we find

$$P_2^2-P_1^2=\frac{24\nu l}{V_0kh^3}Q\frac{T_g}{T}, \tag{2}$$

where Q is the argon flow rate. Based on the theory just presented, we show in Fig. 5 both the average pressure $P=(P_2+P_1)/2$ in the HC as a function of flow rate, and the gas velocity distribution. It may be noted that a low gas velocity near the walls of the cavity is not ideal for the effective sweeping out of sputtered atoms.

C. Reactive-environment sputtering: Al_2O_3

An aluminum target (99.99%) was fabricated for Al_2O_3 thin-film deposition. In conventional dc reactive magnetron sputtering of Al, it is difficult to maintain arc-free deposition and to keep the target in the metallic state. With RE sputtering, our goals were to exclude oxygen from the cavity to achieve arc-free sputtering and high rate deposition of Al_2O_3.

In order to compare the target performance in the oxidized and metallic modes, curves of deposition rate versus oxygen flow rate were measured using a QCM for two cases: (a) oxygen introduced externally to the cathode through a multihole oxygen manifold (RE mode), and (b) oxygen passing through the HC. Figure 6 shows that only a very small amount of oxygen (2–3 sccm) is sufficient to immediately oxidize the target if the oxygen passes through the cathode. The reduced sputter yield results in a dramatic drop in deposition rate. However, in the RE mode, in which the oxygen is introduced outside the cathode, the use of oxygen did not change the cathode metallic state. In this mode, the discharge was perfectly stable and the deposition rate of Al_2O_3 at the center of the substrate was 71 Å/s at 1000 W, 300 mTorr, 4

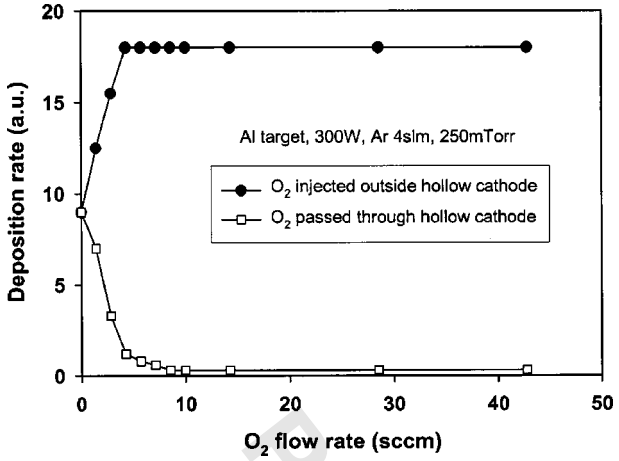

FIG. 6. Comparison of the film deposition rate obtained using an Al target for O_2 injected outside the HC and for O_2 passing through the HC.

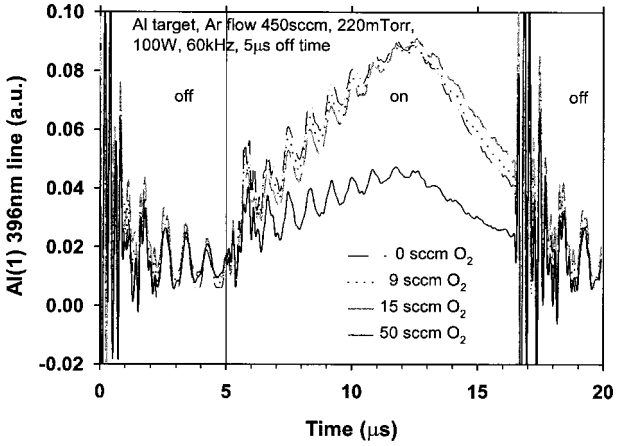

FIG. 7. Time-resolved optical emission from Al(I) line at 396 nm during sputtering of Al with various oxygen flows introduced outside the cathode.

slm Ar, 36 sccm O_2, and $T_s = 120\,^{\circ}\mathrm{C}$. The films were perfectly transparent and had a refractive index of 1.60–1.63 as measured by ellipsometry at 633 nm. Since the atomic weights of Al and O are 26.98 and 16.00, the doubling of the local mass rate in Fig. 6 from 9 to 18 upon introduction of >4 sccm O_2 implies that the stoichiometry of the alumina film is actually $Al_2O_{3.4}$. We also note that the hysteresis region observed in conventional reactive sputtering does not appear in HCS. To summarize, the sputtering rate of the Al target was utterly unchanged by the use of oxygen outside the cathode for flows up to 43 sccm; that is, well in excess of the 5–10 sccm, which is sufficient to fully oxidize the film. These results clearly demonstrate the fundamental advantage of HCS in the RE mode.

Certain combinations of argon and oxygen flow rates will, of course, allow oxygen to backstream into the cathode cavity. This was demonstrated through the acquisition of optical emission spectra. A front-surface Al mirror was set inside the vacuum chamber at EPV at 45° to the optical axis so that the collecting lens and 0.5 m monochromator looked directly into the cavity. The transition lines for Al $(4s^2\mathrm{S} \rightarrow 3p^2\mathrm{P}^0)$ at 396.1 nm and AlO $(B^2\Sigma,\ v=0 \rightarrow X^2\Sigma+,\ v=0)$ at 484.2 nm were recorded as a function of increasing oxygen flow. Three effects were seen. At 1000 sccm Ar, the Al line increases up to an oxygen flow of 3–~4 sccm, perhaps due to level crossing processes. The Al line then decreases while the AlO line continues to increase. Finally, for oxygen flows >20 sccm, the AlO line decreases, which we interpret as the onset of oxygen penetration into the cathode. In the HC system at Stevens, time-resolved measurements of the remote plasma were made. Figure 7 shows the evolution of the 396 nm Al(I) line intensity with increasing oxygen flow into the chamber using 60 kHz pulsed power (5 μs off time, 450 sccm Ar, 220 mTorr). For the smaller O_2 flow rates (0, 9, 15 sccm), the Al(I) profiles are almost identical; at 50 sccm O_2, the intensity profile dropped. Similar behavior was observed for the discharge voltage, indicating that the Al target was partially oxidized.

It may be mentioned that the source at EPV was also used to prepare transparent aluminum nitride (AlN) using N_2 gas supplied externally to the cathode. The mass rate was 1.4 $\mathrm{mg\,min^{-1}}$ at 600 W with Ar and N_2 flows of 2000 and 200 sccm, respectively.

D. TCO deposition: doped ZnO

TCO coatings, such as SnO_2, ITO, and ZnO, have large-area applications for architectural glass, automobiles, displays, and photovoltaics. Conventionally, doped ZnO films are prepared by rf or pulsed dc sputtering of ceramic targets consisting of ZnO with about 2 wt % Al_2O_3.[8] However, the cost of the targets is exorbitant, and the power density that can be applied is limited. More recently, reactive magnetron sputtering from Zn:Al targets has been pursued, although this needs voltage control or closed loop control of oxygen partial pressure to maintain operation in the metal/oxide transition mode.[8,9]

With the goal of avoiding these shortcomings, we have investigated the production of doped ZnO TCOs by pulsed power, RE-HCS. Such a process would offer the advantages of low-cost metal targets and intrinsic process stability. Aluminum and boron were used as dopants. For ZnO:Al film deposition, we have used two large facing targets of Zn with Al end blocks, and, for films of more uniform composition, Zn:Al alloy target pieces (97.5 wt %/2.5 wt %). It was found that many combinations of deposition parameters did not result in conductive films. However, appropriate combinations did. Figure 8 shows some of the results. For the cosputtering of separate Zn and Al targets, the open circles show the as-deposited ZnO:Al film resistivity obtained with various O_2 flow rates. The other parameters were fixed at 100 W, 2 slm Ar, 200 mTorr, 3.5 cm, and $T_s = 120\,^{\circ}\mathrm{C}$. The oxygen flow rate is seen to be critical, with a minimum in the resistivity ($6.7\times10^{-4}\,\Omega$ cm) occurring near 100 sccm. In other experiments, a resistivity of $4.9\times10^{-4}\,\Omega$ cm was achieved. The films have very low optical absorption in the visible region. For ZnO:Al films deposited from the alloy target, a similar minimum in resistivity was observed at 140 sccm O_2, the value being $1.2\times10^{-3}\,\Omega$ cm. The other parameters

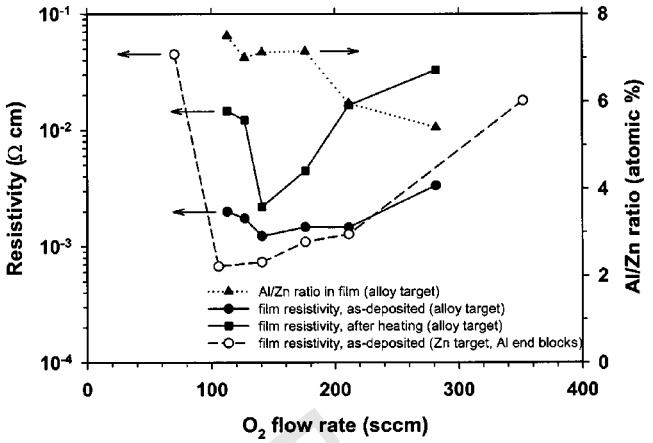

FIG. 8. Properties of ZnO:Al films (resistivity and Al content) as a function of oxygen flow rate.

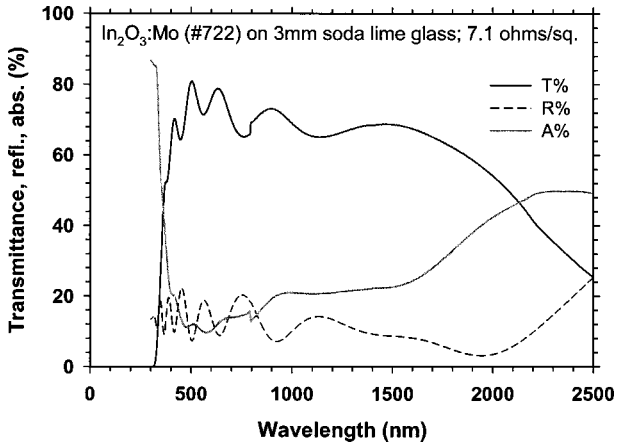

FIG. 9. Optical spectra for a 7.1 Ω/□ molybdenum-doped indium oxide film produced by RE-HCS.

were 300 W, 2 slm Ar, 300 mTorr, 3.5 cm, and $T_s = 150\,^{\circ}\mathrm{C}$, and the film thickness was about 300 nm. The Al concentration was measured by ICP, and Fig. 8 shows that the Al/Zn atomic ratio decreases for the higher O_2 flows.

Quite conductive ZnO films can be produced without the addition of a dopant, the conductivity resulting from O vacancies or Zn interstitials. Such films are unstable upon heating, while the conductivity resulting from substitutional dopants is unchanged. After heating the alloy-target ZnO:Al films on a hotplate to 220 °C in air for 20 min, their resistivity increased, while a conventional rf-sputtered sample was unaffected. The film prepared at the optimum oxygen flow increased from 1.2×10^{-3} to $2.0\times10^{-3}\,\Omega$ cm, whereas the resistivity of other films increased by up to a factor of 10. In later work, some ZnO:Al films were produced at somewhat higher pressure whose resistivity increased by only 50% under the more aggressive heating schedule of 270 °C for 40 min.

To deposit ZnO:B films, the target was Zn, and a gas mixture of 5% B_2H_6 in Ar was used as the boron source. In these experiments, the gas mixture was injected by an independent manifold outside the HC, with oxygen supplied from the usual oxygen manifold. The dependence of ZnO:B film resistivity on O_2 flow rate was determined for B_2H_6 mixture flows of 0, 2, and 4 sccm. The deposition parameters were 300 W, 2 slm Ar, 300 mTorr, and $T_s = 165\,^{\circ}\mathrm{C}$. Overdoped and nondoped films exhibited a higher resistivity than midlevel doped films. As with ZnO:Al, the O_2 flow rate strongly affected the resistivity, with larger flow rates leading to higher resistivity. A minimum resistivity of $5.7\times10^{-4}\,\Omega$ cm was achieved for ZnO:B at a boron content of 0.5–0.8 at. %. Other ZnO:B films were produced at a sputtering power of 900 W. Typically, heating ZnO:B films in air to 270 °C for 40 min resulted in a 25% increase in resistivity, and the stability of ZnO:B was in general superior to that of ZnO:Al. Two ZnO:B films were found to be completely stable.

E. TCO deposition: In_2O_3:Mo

As a further example of the application of this technology, we present a few results obtained regarding the preparation of the transparent conducting oxide In_2O_3:Mo. We have confirmed that Mo is an *n*-type dopant for In_2O_3, as originally reported by Meng *et al.* for films produced by reactive evaporation.[10] In that work, it was reported that Mo^{6+} substituted for In^{3+}, suggesting the possibility of three conduction electrons per dopant atom. More recently, In_2O_3:Mo films have been prepared by rf magnetron sputtering.[11]

In our initial work, RE sputtering with two facing indium targets and various configurations of smaller molybdenum pieces was used to deposit films of In_2O_3:Mo having varying Mo concentrations onto heated, stationary substrates. Deposition parameters were 2 slm Ar, 0.3 slm O_2, 100 W (at 100 kHz, 150 mTorr, and $T_s = 300\,^{\circ}\mathrm{C}$. The Mo content was measured by ICP. The lowest resistivity films were obtained for a Mo/In ratio (atomic) of 1.2%, with $1.9\times10^{-4}\,\Omega$ cm being the minimum value obtained. It is of interest that this conductivity was obtained at the modest substrate temperature of 300 °C. Other Mo/In ratios yielded the following resistivities ($10^{-4}\,\Omega$ cm): 0%, 50.1; 3.9%, 2.2; 7.2%, 10.5; 17.8%, 104.

More uniform samples of In_2O_3:Mo were produced by translating the substrate using a rack-and-pinion drive (2 slm Ar, 0.2 slm O_2, 180 W, 150 mTorr, 300 °C). Figure 9 shows the optical transmittance, reflectance, and absorbance of a

TABLE III. Deposition efficiency of magnetron and hollow cathode sources.

Deposition method	Material	Dynamic rate[a] (nm m min^{-1})	Deposition efficiency (10^{-3} nm m^2 min^{-1} W^{-1})
Magnetron (EPV)	Cu	21	10.4
HC (EPV)	Cu	25	3.4
Magnetron[b]	Al_2O_3	11.5	2.8
HC (EPV)	Al_2O_3	10	1.4
HC[c]	Al_2O_3	27	0.71

[a]Depends on process power.
[b]See Ref. 12.
[c]See Ref. 13.

TABLE IV. Comparison of sputtering-based processes for production of ZnO:Al films.

Method	Target	Substrate temp. (°C)	Deposition rate (Å s^{-1})	Dynamic rate (nm m min^{-1})	Resistivity (10^{-4} Ω cm)
RF magnetron (600 W, 38 cm)	Ceramic	Unheated	5.8	3.5	4.5
Pulsed magnetron (2100 W, 56 cm)	Ceramic	150	42.0	25.4	12.5
Hollow cathode (900 W, 10 cm)	Metal	90	67.0	17.0	5.7

450-nm-thick, 7.1 Ω/sq., In_2O_3:Mo film having a resistivity of $3.2\times10^{-4}\,\Omega$ cm. That the long-wavelength fall-off in transmittance does not occur until 1500 nm and beyond is suggestive that the observed conductivity is obtained by virtue of a high mobility/lower carrier concentration combination. The plasma wavelength is estimated to be about 2300 nm. Further results in this area will be published separately.

F. Scaling, deposition efficiency, and process comparisons

During the scaling up of these HC sources, it is of interest to compare the performance of cathodes of different sizes and designs. Since power (P) and gas flow rate (F) are the principal determinants of deposition rate, we may define an efficiency η_{PF} for a given target material equal to mass rate/$(P\times F)$. For the Stevens and EPV cathodes with Cu targets, the mass rates are 1.2 and 26.7 mg min^{-1} at flow rates of 0.9 and 4.0 slm and at powers of 0.2 and 1.0 kW respectively. Remarkably, η_{PF}(Cu) turns out to be 6.7 mg sl^{-1} kW^{-1} for both of the cathodes, suggesting this quantity should be invariant upon scaling the cathode. For Al_2O_3 deposited with the EPV cathode, η_{PF} is 1.3 mg sl^{-1} kW^{-1}.

We now compare the deposition efficiency of the HC source with that of a conventional magnetron source. Deposition efficiency η_d is defined as the total film volume deposited per minute and per watt of power, or film volume per unit energy dissipated. The units are nm m^2 min^{-1} W^{-1} (occasionally nm m^2 J^{-1}). The deposition efficiency is related to the dynamic deposition rate R_d obtained with moving substrates by the equation $\eta_d = R_d\times L/P$, where L is the cathode length, and P is the sputtering power. (R_d, with units nm m min^{-1}, is defined as film thickness×substrate speed). Table III shows η_d for Cu and Al_2O_3 from different laboratories. On an energy basis, the deposition efficiency of magnetron sources is 2–3 times that of HC sources. From the point of view of throughput, however, what is most important is the achievable dynamic deposition rate, and this depends on the power per unit length that the cathode can sustain. We have not yet explored these limits for hollow cathode sources. For magnetron ZnO, an R_d of 60 nm m min^{-1} per cathode has been achieved with ceramic targets,[14] and 80 nm m min^{-1} in a reactive mode with Zn:Al targets.[9]

Finally, we assess the RE sputtering process for ZnO:Al relative to other sputter-based processes. This is done in Table IV for three processes in use at EPV. The pulsed magnetron process utilizes substrate translation, and the 42 Å s^{-1} deposition rate is the instantaneous rate averaged over the 10 cm target width. The data for the HC process was obtained with a 2.5 cm cavity width, 900 W, 2 slm Ar, 56 sccm O_2, and 300 mTorr. It can be seen that the HC process offers high film quality, low target cost, and a dynamic deposition rate for a single cavity approaching that currently used in the magnetron process.

IV. CONCLUSIONS

We have outlined the principles of reactive-environment sputtering using a linear and scalable hollow cathode source. The key advantage of this method is the ability to sputter in a fully metallic mode while forming compounds on the substrate. This was demonstrated through the deposition of Al_2O_3 and AlN. The method has been applied to the production of the transparent conductors ZnO:Al, ZnO:B, and In_2O_3:Mo. We found the TCO properties to be sensitive to the details and uniformity of the oxygen supply. It is believed that the utilization of the reactive gas depends on its degree of dissociation in the cathode afterglow. The features of the method include: high plasma density, high deposition rate, arc-free operation, easy and controllable deposition of insulating materials, choice of minimal sputtering damage or low-energy ion bombardment, low heat input to substrate (if desired), high target utilization, and scalability for industrial application. It is anticipated that this type of source and the method described will find commercial applications in the preparation of compound films for transparent conductors, superconductors, semiconductors, resistors, ferroelectrics, barrier coatings, tribological coatings, and wear-resistant coatings.

ACKNOWLEDGMENTS

This work was largely supported by an ATP award from NIST to Energy Photovoltaics, Inc., agreement no. 70NANB0H3031. The authors thank R. Lyndall for source construction, and Dr. T. J. Coutts (NREL) and Y. Yoshida (Colorado School of Mines) for measurement of the In_2O_3:Mo optical spectra.

[1]V. I. Kolobov and L. D. Tsendin, Plasma Sources Sci. Technol. **4**, 551 (1995).
[2]K. Ishii, J. Vac. Sci. Technol. A **7**, 256 (1989).

[3]H. Koch, L. J. Friedrich, V. Hinkel, F. Ludwig, B. Politt, and T. Schurig, J. Vac. Sci. Technol. A **9**, 2374 (1991).
[4]T. ung and A. Westphal, Surf. Coat. Technol. **59**, 171 (1993).
[5]Th. Jung, T. Klber, and V. v.d. Heide, Surf. Coat. Technol. **86–87**, 218 (1996).
[6]C. Paduraru, K. Becker, A. Belkind, A. E. Delahoy, S. Y. Guo, and J. Lopez, *Proc. 26th Intl. Conf. on Phenomena in Ionized Gases*, Greifswald, Germany, 2003, Vol. I, p. 35.
[7]C. Paduraru, A. Belkind, K. H. Becker, J. Lopez, A. E. Delahoy, and S. Y. Guo, *Proc. 46th SVC Annual Technical Conference*, 2003, p. 130.
[8]A. E. Delahoy and M. Cherny, Mater. Res. Soc. Symp. Proc. **426**, 467 (1996).
[9]B. Szyszka, T. Höing, X. Jiang, A. Bierhals, N. Malkomes, M. Vergöhl, V. Sittinger, U. Bringmann, and G. Bräuer, *Proc. 44th SVC Annual Technical Conference*, 2001, p. 272.
[10]Y. Meng, X. L. Yang, H. Chen, J. Shen, Y. M. Jiang, Z. J. Zhang, and Z. Y. Hua, Thin Solid Films **394**, 219 (2001).
[11]Y. Yoshida, T. Gessert, C. Perkins, and T. Coutts, J. Vac. Sci. Technol. A **21**, 1092 (2003).
[12]M. Kharrazi Olsson, K. Macak, and W. Graf, Surf. Coat. Technol. **122**, 202 (1999).
[13]M. Höfer, A. Jung, Th. Jung, H.-U. Kricheldorf, and F. Schmidt, *Proc. 43rd SVC Annual Technical Conference* 2000, p. 287.
[14]C. May, J. Strümpfel, and D. Schulze, *Proc. 43rd SVC Annual Technical Conference*, 2000, p. 137.

PROOF COPY 050404JVA